THE ASTROPHYSICAL JOURNAL, 442:358–365, 1995 March 20

THE DIM INNER ACCRETION DISK OF THE QUIESCENT BLACK HOLE A0620−00[1]

JEFFREY E. MCCLINTOCK,[2] KEITH HORNE,[3] AND RONALD A. REMILLARD[4]
Received 1993 December 3; accepted 1994 September 28

ABSTRACT

We observed the X-ray nova A0620−00 with the *Hubble Space Telescope* (*HST*) Faint object Spectrograph 16 yr after its 1975 outburst. We present a single spectrum (1250–4750 Å), which is approximately an average over a full 7.8 hr orbital cycle of the source. The continuum can be fitted approximately by a blackbody model with $T = 9000$ K and a small projected source area, which is ∼1% of the expected area of the accretion disk. A0620−00 is faint in the far-UV band; its luminosity is comparable to the luminosity of a quiescent dwarf-nova accretion disk (i.e., excluding the white dwarf). By analogy with dwarf novae, the optical luminosity of the disk ($M_v \approx 7$) and the orbital period of A0620−00 imply that the rate of mass transfer onto the outer disk in $\dot{M}_d \sim 10^{-10}\ M_\odot$ yr^{-1}.

We also observed A0620−00 with the *ROSAT* PSPC X-ray detector for 3×10^4 s and detected a faint source (5 σ) at the location of the X-ray nova. For an assumed blackbody spectrum the source temperature and luminosity are ∼0.16 keV and 6×10^{30} ergs s^{-1}, respectively ($d = 1$ kpc). This luminosity implies that the rate of mass transfer into the black hole is extraordinarily small: $\dot{M}_{BH} < 5 \times 10^{-15}\ M_\odot$ yr^{-1}. The much larger mass transfer rate onto the outer disk, and the UV/X-ray faintness of the inner disk confirm key predictions of the disk instability model for the nova outburst of A0620−00 published by Huang and Wheeler and by Mineshige and Wheeler.

Subject headings: accretion, accretion disks — binaries: close — black hole physics — stars: individual (A0620−00) — X-rays: stars

1. INTRODUCTION

In the fall of 1975, the X-ray nova A0620−00 was the brightest celestial X-ray source. During outburst it was identified with a blue star of 12th magnitude. Fifteen months later the optical counterpart had returned to its preoutburst brightness, $V = 18.3$. Its quiescent spectrum was found to consist of two components which are about equally bright in the V band: an approximately K5V stellar spectrum and an emission-line component that was attributed to an accretion disk (Oke 1977; Whelan et al. 1977; Murdin et al. 1980).

Photometry and spectroscopy in quiescence revealed a 7.75 hr orbital period, a large velocity amplitude for the K5V secondary, and a corresponding mass function of approximately 3 $M_\odot$ (McClintock & Remillard 1986). This large mass function established A0620−00 as a leading black-hole candidate, a conclusion that has been confirmed and extended (Johnston, Kulkarni, & Oke 1989; Haswell & Shafter 1990; McClintock & Remillard 1990; Johnston & Kulkarni 1990; Haswell et al. 1993; Marsh, Robinson, & Wood 1994).

In this paper we focus on the optical, UV, and X-ray emission from the quiescent accretion disk. The optical luminosity of the quiescent disk is approximately the same as that of the K5V secondary, $M_v \approx 7$ (Oke 1977). This luminosity is also a typical value for a dwarf nova disk (with $P_{orb} \sim 8$ hr) that is powered by a mass accretion rate of $\dot{M} \sim 10^{-10}\ M_\odot$ yr^{-1} (Warner 1987). Consequently, in analogy with dwarf novae, McClintock (1986) pointed out that one might expect for A0620−00 a substantial mass flow rate through the disk and onto the compact object, and a corresponding quiescent X-ray luminosity of $\sim 10^{35}$ ergs s^{-1}. He noted as a puzzle, however, that the observed 0.2–2 keV X-ray luminosity is less than 10^{32} ergs s^{-1} (Long, Helfand, & Grabelsky 1981). One reason for this absence of X-rays was suggested by de Kool (1988). Since the maximum temperature in a steady black-hole disk scales as $M_x^{-1/2}\dot{M}^{1/4}$ (cf., Fu & Taam 1990), de Kool argued that a quiescent disk around a massive black hole might be so cool (e.g., $T_{max} \approx 60$ eV for $M_x = 7\ M_\odot$ and $\dot{M} = 10^{-11}\ M_\odot$ yr^{-1}) that only a tiny and undetectable fraction of the flux would penetrate the interstellar medium.

Another possible reason for the absence of quiescent X-ray flux is suggested by the disk instability model (Cannizzo 1993, and references therein), which has been tailored explicitly for A0620−00 by Huang & Wheeler (1989) and Mineshige & Wheeler (1989). Their models assume a steady rate of mass transfer onto the outer disk of $\dot{M} \sim 3 \times 10^{-11}\ M_\odot$ yr^{-1}, which is the rate inferred from the energy released in the 1975 outburst and the time interval between outbursts (58 yr). In this model, only a tiny fraction ($\sim 10^{-5}$) of the matter impinging on the outer disk steadily makes its way to the compact object; consequently, the predicted X-ray luminosity is minuscule. The great bulk of the disk material is dammed up for decades at intermediate radii until it is suddenly released by a thermal instability, which is accompanied by a large increase in viscosity.

In § 2 we discuss the UV/optical observations obtained with *HST*, the X-ray observations obtained with *ROSAT*, and supporting optical observations, which were performed at three ground-based observatories. A UV/optical spectrum and X-ray spectral parameters are presented in § 3. In § 4, the spectra are discussed and used as evidence to support the disk

[1] Based on observations with the NASA/ESA Hubble Space Telescope obtained at the Space Telescope Science Institute, which is operated by AURA, Inc., under NASA contract NAS5-26555.

[2] Harvard-Smithsonian Center for Astrophysics, 60 Garden St., Cambridge, MA 02138; jem@cfa.harvard.edu.

[3] Sterrekundig Instituut Utrecht, Postbus 80000, 3508 TA Utrecht, Netherlands. E-mail: horne@fys.ruu.nl; also Space Telescope Science Institute; horne@stsci.edu.

[4] Center for Space Research, Room 37-595, Massachusetts Institute of Technology, Cambridge, MA 02139; rr@space.mit.edu.

instability model. The last section comments on the tranquility of the quiescent state.

2. OBSERVATIONS AND ANALYSES

2.1. *HST Far-UV/Optical Spectroscopy*

A total of 10 spectra were recorded sequentially commencing on 1992 January 4 at 10:24 UT using the Faint Object Spectrograph (FOS), blue Digicon detector, and a single 1".0 diameter aperture. Six exposures, each of duration 23.6 minute, were obtained using the G160L grating (G), and four additional 3.8 min exposures were obtained using the blue prism (P). The exposures were frequently separated by an Earth occultation (e). The observing sequence was: PeGeGPeGeGPeGeGP. Each grating and prism exposure was further subdivided into 46 s subexposures via the RAPID model. The total on-source observing time was 2.36 hr with the grating and 0.25 hr with the prism. The observations, which took place regularly during a 10.2 hr interval, provided fairly uniform coverage of a complete 7.8 hr orbital cycle of the source. The grating spectra cover the wavelength range 1250–2400 Å and the prism spectra cover 2200–4750 Å. The grating provides a dispersion of 7 Å per diode; the dispersion of the prism varies from 12 Å per diode at 2400 to 120 Å per diode at 4750 Å. Because the source was faint we present one composite spectrum (prism plus grating), which is averaged over all the observations.

We used the standard IRAF data analysis packages and standard techniques in reducing the data. There were, however, some complications. The source flux in the far-UV was much lower than we had expected, and therefore it became important to obtain the best possible measure of the background count rate in the ultraviolet. Unfortunately we do not have a direct measure of the background rate, which is due to cosmic rays, because we observed the source continuously with a single aperture. Furthermore, the model background provided by the STScI "pipeline" processing seriously underestimates the observed background level. Nevertheless, as shown in Figure 1, we derived a reasonable estimate of the true background rate by determining the signal level over selected, unilluminated portions of the detector array, which is comprised of 512 diodes = 2064 pixels. The raw G160L grating data are shown in Figure 1*a*. The upper smooth curve represents the adopted background level. Similarly, the raw prism data and the adopted background level (upper smooth curve) are shown in Figure 1*b*.

We examined and rejected the idea that scattered red light from A0620−00 might contribute significantly to the grating spectrum shown in Figure 1*a*. Using the known optical spectrum of A0620−00 (e.g., Oke 1977) and the results summarized in Blair, Davidsen, & Uomoto (1989), we find a small contribution to the count rate due to scattered light that is less than 3% of the cosmic-ray–induced rate.

The wavelength and flux calibrations were obtained from the standard data products in the usual way. The grating spectrum was dereddened using the interstellar extinction law of Cardelli, Clayton, & Mathis (1989) and a reddening of $E(B-V) = 0.35$ (Wu et al. 1983; also, see Oke & Greenstein 1977 and Whelan et al. 1977). The prism spectrum was similarly reduced to standard form and dereddened. In the final step of forming a single merged spectrum, the prism and grating fluxes were averaged in the range of overlap (2200–2400 Å).

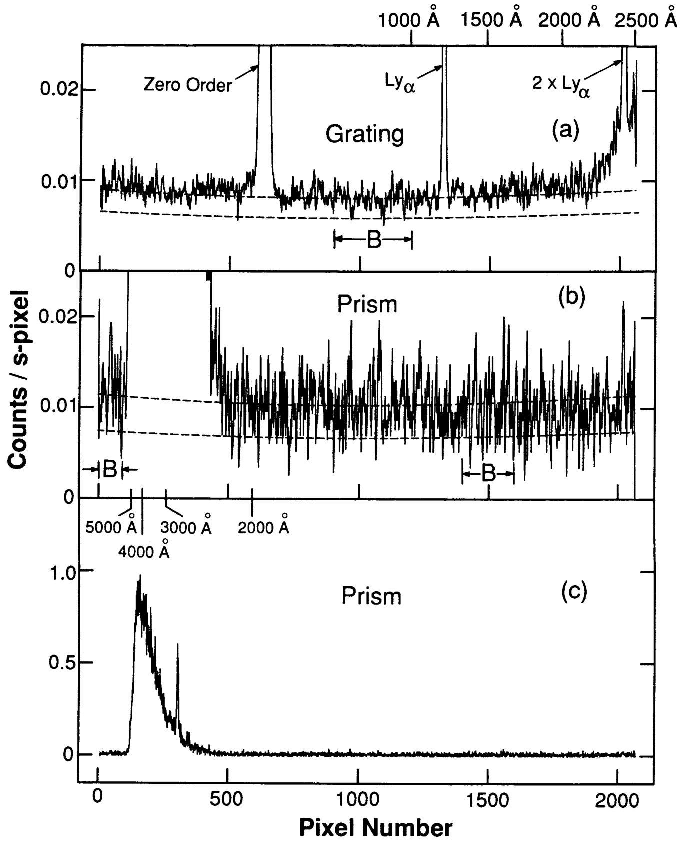

FIG. 1.—Raw counting rate data with the background rate included. (*a*) G160L grating data averaged over the entire 2.36 hr of observation and smoothed by 5 pixels. The adopted background region consists of pixels 901–1200 and is marked "B." The model background spectrum adopted by us is represented by the upper smooth curve; it was derived by scaling up the STScI standard ("c7") background spectrum (*lower curve*) by a factor of 1.374 to match the count rate in the background region. The emission line at λ2430 is Lyα in second order; second order overlaps first order longward of 2300 Å, but contributes only a few percent to the continuum flux. Note the wavelength scale in the upper right of the figure. (*b*) Blue prism data averaged over all the observations and smoothed by 5 pixels. The adopted background regions marked "B" are pixels 1–100 and 1401–1600. The upper smooth curve corresponds to our adopted background spectrum. It was derived by scaling up the STScI standard ("c7") background spectrum by a factor of 1.538 to match the average count rate in the background regions. (c) A replot of the prism data with the vertical scale greatly compressed. A crude wavelength scale, which also applies to (*b*), is shown. Note the Mg II λ2800 line centered at about pixel 300.

2.2. *HST UV Photometry*

We used the light reflected from the G160L grating at zero order (see Fig. 1*a*) to derive an orbital light curve for A0620−00. The grating response at zero order extends from 1200 to 5500 Å (FWHM = 1900 Å) and is centered at about 3400 Å (Horne & Eracleous 1993). Thus the light curve of the zero-order flux is chiefly due to the accretion disk with a minor contribution from the K star. The light curve, which is shown in Figure 2, consists of 186 count rate measurements made over an interval of 8.4 hr.

The light curve shows significant flickering with amplitudes of up to ∼15% on a timescale of a few minutes and ∼20% on the *HST* orbital timescale of 1.5 hr. We investigated the possibility that the flickering is instrumental. We plotted the

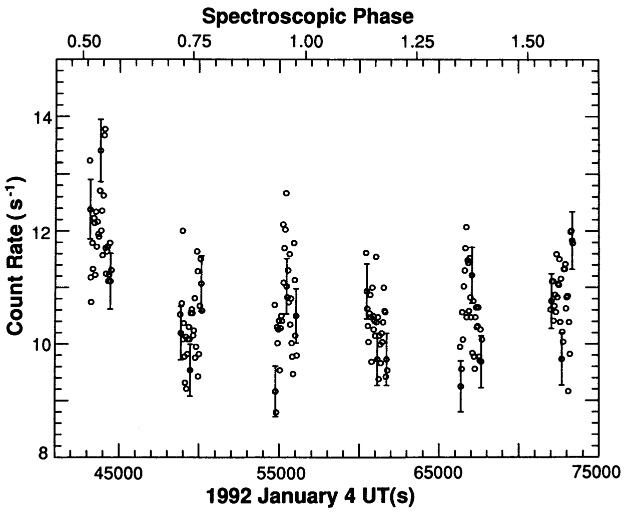

FIG. 2.—A broadband light curve showing primarily the orbital variation of the accretion disk over a full orbital cycle (see text). Phase 1.0 corresponds to the time of maximum velocity of the secondary. The count rates are divided into six groups, and each group provides 24 minutes of continuous coverage. The groups are separated by 1.5 hr, the time between *HST* orbits. Approximately 400–600 counts were detected in each 46 s exposure; the uncertainties due to counting statistics are indicated by several representative error bars. Note that source variability on a timescale of a few minutes is evident, especially for the data points near 55,000 s UT.

smooth orbital variations in both the telescope focus and the *y*-component of Earth's magnetic field, and overplotted the count rate data. We searched visually for correlations; none were found. Similarly, the Fine Guidance Sensor data showed that the variations in count rate were not correlated with spacecraft motion; moreover, the spacecraft motion during each 24 min interval of continuous observation was very small ($\lesssim 0''.02$). Thus it appears probable that the flickering is due to the source, although we cannot completely rule out an instrumental origin.

2.3. *Ground-based Photometry and Spectroscopy*

The red end of the *HST* spectrum (4000–4750 Å) contains a contribution from the secondary star. We used ground-based photometric data, which were obtained 2 days prior to the *HST* observations, to quantify and subtract this contribution from the secondary star in order to isolate the spectrum of the accretion disk.

Two days before the *HST* observations, on 1992 Jan 2 (3–11 hr UT), we obtained 127 CCD images of the field using a blue (B-460) filter and the 1.3 m telescope at the MDM Observatory. The light curve derived from these data is very similar in average intensity and in appearance to the double-humped, blue light curves we have obtained almost every year since 1984. The phase-averaged intensity of the light curve 2 days prior to the *HST* observations corresponds to a value of 0.57 in Figure 1*a* of McClintock & Remillard (1986). (The intensity scale is normalized to the intensity of a local reference star at an effective wavelength of 5500 Å). This value corresponds to a typical quiescent state in which both the K star and the accretion disk are comparably bright near 5500 Å.

Several methods have been used to decompose the spectra of the secondary star and the accretion disk in the case of A0620−00 (e.g., Oke 1977; McClintock & Remillard 1986). Here we report on the analysis of six spectroscopic data sets obtained between 1985 January and 1991 January. Our method (which is a modification of the one described in McClintock & Remillard 1986) determines a K-star fraction by finding the best least-squares match between a spectrum of A0620−00 and a variety of model spectra, which are described below. At each epoch we created a summed spectrum of A0620−00 in the rest frame of HII3019, a K5V standard star. This summed spectrum and the spectrum of the standard star were both smoothed to an effective resolution of 5 Å to eliminate differences in the widths of the lines due to the rotation of the secondary and to the changes in its orbital velocity that occurred during a typical 20 minute exposure. (The results, which are discussed below, are insensitive to the degree of smoothing over the range 3–12 Å.) We selected the wavelength range 5150–5300 Å, which is populated by the strongest absorption lines, and flattened the continuum spectra of both A0620−00 and the standard star. A few dozen model spectra were created by adding to the standard-star spectrum a number of different constant terms, each of which corresponds to a different contribution to the total light by the accretion disk. The continuum levels in all the spectra were normalized to unit intensity, and a least-squares comparison was made between one of the summed spectra of A0620−00 and each of the model spectra in turn. The results expressed in terms of the fraction of light contributed by the K-star secondary at 5225 Å (or 6425 Å) are given in Table 1. They indicate that the K-star fraction at 5225 Å appears to be roughly constant during the period 1985–1990 at $\sim 58\%$, which agrees with the result obtained in 1976 November by Oke (1977).

Extensive photometric data were obtained within a month of four of the spectroscopic observations listed in Table 1. For each of these epochs, the data were used to derive a relationship between the phase-averaged intensity of the light curve and the spectroscopic K-star fraction, under the assumption that the luminosity of the K star does not vary. Using this relationship, we find that *the* K *star contributed* $55 \pm 10\%$ *of the light at* 5225 Å *during the HST observations of* A0620−00. We conclude that the behavior of A0620−00 in the blue was very ordinary 2 days prior to the *HST* observations.

We note that a larger K-star contribution, $83 \pm 4\%$ (4400–5200 Å), was derived for this time period by Marsh et al. (1994). The difference between their result and ours is probably due to the choice of template star. Their star, which they describe as "variously listed as a K3 or K4 dwarf," presumably has weaker absorption lines than our K5 dwarf. Consequently, in order to match the equivalent widths of the lines in the spectrum of A0620−00, their template star must contribute a larger fraction of the observed continuum. An examination of the spectrum of the accretion disk, which is presented in § 3.1, shows that if their value were adopted, it would imply a fainter disk

TABLE 1

FRACTION OF THE TOTAL LIGHT DUE TO THE SECONDARY STAR

UT Date	Telescope	Bandpass	K-Star Fraction
1985 Jan 17...........	KPNO 4m	5150–5300	0.44 ± 0.08
1985 Dec 11	MMT	5150–5300	0.57 ± 0.04
1987 Nov 17–18......	MMT	5150–5300	0.63 ± 0.05
1988 Feb 13	MMT	5150–5300	0.71 ± 0.12
1989 Feb 4............	MMT	5150–5300	0.57 ± 0.07
1991 Jan 11[a]	MMT	6350–6500	0.73 ± 0.05

[a] The shortest wavelength observed at this epoch was 6200 Å.

($M_v \approx 8$) with a spectrum that falls rapidly in flux with increasing wavelength between 3000 and 5000 Å. These changes, however, would not materially affect the conclusions presented in this work. Moreover, the uncertainty in the *absolute* value of the K-star fraction does not affect our conclusion that the *relative* value was fairly constant between 1985 and the time of the *HST* observations.

2.4. *ROSAT X-Ray Observations*

We observed the field of A0620−00 with the *ROSAT* PSPC imaging detector for 3×10^4 s. The observations, which were made during 5 days in 1992 (March 10 and March 24–27), provide good phase coverage of the 7.8 hr orbital cycle of A0620−00. Production processing of the data by the *ROSAT* Science Data Center with the Standard Analysis and Software System yielded a Final Source List containing 28 sources, which are located within the central 30′ × 30′ of the field of view. One of these sources is located 11″ from the precise optical position of A0620−00. Moreover, after correcting for systematic errors by comparing the X-ray positions of three sources (located within 30′ of the telescope axis) to their precise optical positions, we found that the positions of A0620−00 and the X-ray source differed by only 8″. If we assume that the positional uncertainty for a faint source is $\lesssim 10''$, then the a priori probability that any one of the 28 sources would coincide with the position of A0620−00 to within 10″ is $\lesssim 0.001$. Thus it is very likely that we have detected the quiescent X-ray nova.

We determined the count rate of A0620−00 using the PROS software (an X-ray data analysis package that runs under IRAF) and a single X-ray image that incorporates the entire 3×10^4 s of data. The source counts were extracted from a circular region centered on the source with a radius of 56″; the background rates were extracted from a concentric annular region with inner and outer radii of 80″ and 160″, respectively. The total number of net source counts detected in 3×10^4 s was 39 ± 8 counts in PHA channels 10–24 in the SASS 34 binning scheme. (In the 256 channel scheme the corresponding PHA range is channels 37–140; the nominal energy range is 0.4–1.4 keV.) In order to perform a spectral analysis with so few counts, we used the maximum-likelihood method (Cash 1979). We assumed, furthermore, that the disk radiates as a blackbody, as suggested by theoretical studies of classical and relativistic disks (e.g., Fu & Taam 1990), and we fixed the interstellar column density at $N_H = 1.6 \times 10^{21}$ cm^{-2}, which corresponds to $E(B-V) = 0.35$ (see § 2.1; Heiles, Stark, & Kulkarni 1981).

We used the X-ray spectral fitting package XSPEC to constrain the blackbody temperature and source luminosity. In a likelihood analysis it is not permissable to subtract the background. Therefore, we fitted the source and background regions simultaneously using PHA channels 10–24 and five parameters, two for the source (with N_H fixed) and three for the background. Both the background spectrum and the source spectrum were well fitted by blackbody models. With the background parameters fixed at their best values ($kT = 0.07$ keV; $N_H = 1.2 \times 10^{21}$ cm^{-2}), we used the measured values of the source parameters and the XSPEC routine "fakeit" to simulate 1000 synthetic source spectra. Fitted parameters (temperature and luminosity) were derived for each of these spectra in exactly the same way they had been derived for the observed spectrum. Confidence regions corresponding to the distribution of these parameters are shown in Figure 3. The following are the best-fit values of the source temperature and luminosity for $d = 1$ kpc):

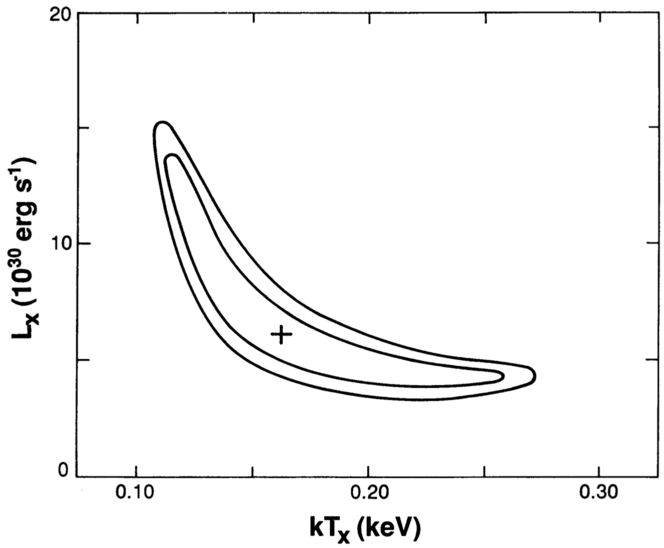

FIG. 3.—Results obtained by fitting a blackbody spectrum to the X-ray data. The cross is located at the best-fit values of the parameters kT_x and L_x. Contours corresponding to 68% and 90% confidence levels are shown. A distance of 1 kpc is assumed.

$$kT_x = 0.16^{+0.10}_{-0.05} \text{ keV}$$

$$L_x = 6^{+8}_{-2} \times 10^{30} \text{ ergs s}^{-1}$$

These results are fairly insensitive to the value of the column density assumed above. For example, consider a 50% larger value, $N_H = 2.4 \times 10^{21}$ cm^{-2}, which is the value predicted for $E(B-V) = 0.35$ by Gorenstein (1975). In this case, the best-fit temperature would be slightly lower ($kT_x = 0.15$ keV) and the best-fit luminosity would be 60% greater than the values given above.

3. RESULTS

3.1. *Far-UV/Optical Spectrum*

3.1.1. $\lambda > 2200$ Å

The spectrum of A0620−00 is shown in Figure 4*a*. Longward of ∼2200 Å, the continuum level is well established and does not depend significantly on uncertainties in the background (§ 2.1). It is useful to compare our optical spectrum to the spectrum of A0620−00 obtained 15 months after outburst by Oke (1977). A smoothed version of his spectrum is shown in Figure 4*a*. A comparison of the spectra implies that A0620−00 brightened by ∼0.3 mag between the 1977 and 1992 observations. This modest degree of variability is not surprising, given the known ellipsoidal and secular variability of A0620−00 (Haswell et al. 1993; McClintock & Remillard 1990) and the 15 yr interval between the observations. The comparison of the spectra provides strong evidence that A0620−00 was adequately centered in the 1″0 FOS aperture.

The spectrum of the accretion disk is shown in Figure 4*b*. It was derived by subtracting the scaled spectrum of a K5 dwarf from the spectrum of A0620−00 (see the caption for Fig. 4). The prominent feature in the spectrum of the disk is Mg II λλ2796, 2803, which has an equivalent width of 140 ± 20 Å and a line width of 36 ± 4 Å. If we assume a Gaussian profile, and

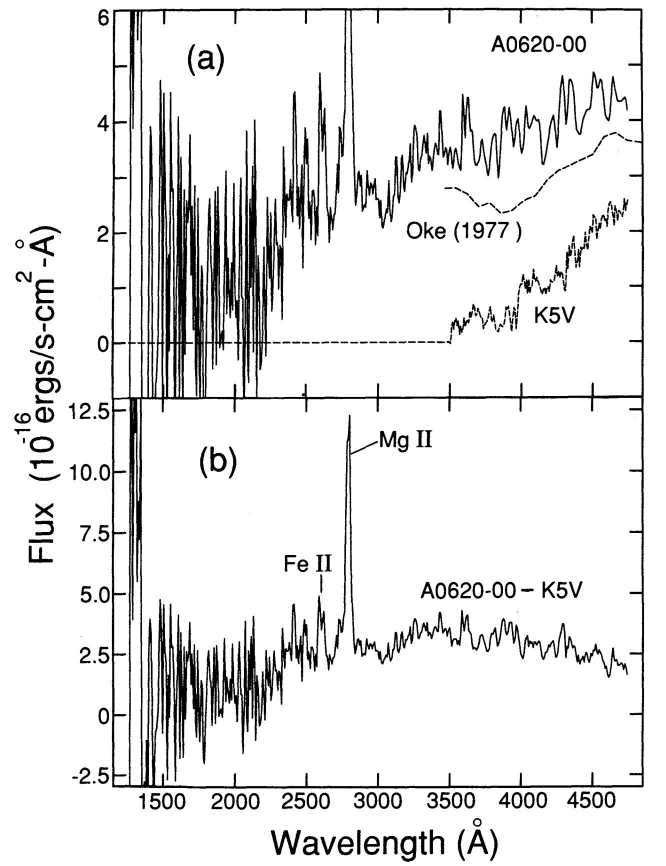

FIG. 4.—(*a*) The dereddened and unsmoothed spectrum of A0620−00 (*solid line*). For comparison in the optical we show a smoothed version of Oke's (1977) spectrum for $\lambda \geq 3460$ Å. Also shown is the dereddened spectrum of a K5 dwarf (SAO 76803; Jacoby, Hunter, & Christian 1984). The K star's flux has been normalized to correspond to the relative intensity given in § 2.3. The flux of the K dwarf is very small below 3500 Å and we ignore it (e.g., Wu et al. 1991; see their spectrum of HD 219134). (*b*) The dereddened spectrum of the accretion disk obtained by subtracting the K5V spectrum from the spectrum of A0620−00 (see *a*). There are two statistically significant spectral features: Mg II λ2800 and Fe II λ2600 (see § 3.1.1). We disregard the intense, broad ($\approx$ 80 Å) feature centered at $\approx$1300 Å. It is an artifact due to our limited knowledge of the particle-induced background (§ 2.1). The feaure is identifiable in the raw grating data (Fig. 1*a*) as a broad but small bump centered near pixel number 1375. Its prominence here is due to the large (3.4 mag) correction for reddening at 1300 Å that has been applied.

an adopted instrumental resolution of 27 Å (for an assumed instrumental source size of 0".5; Kinney 1992) we find FWHM(Mg II) = 2600 ± 700 km s^{-1}, which is consistent with the widths of the Balmer lines (McClintock & Remillard 1986; Marsh et al. 1994). The only other significant feature is Fe II $\lambda\lambda$2586–2631, which has an equivalent width of 45 ± 15 Å. Notably absent from the spectrum is the C IV λ1549 resonance line. This line is very prominent in emission in the spectra of most dwarf novae, where it is produced by photoionization by the UV photons from the white dwarf and the accretion disk. Its equivalent width is typically a few times the equivalent width of the Mg II λ2800 line (la Dous 1991). The absence of this line in our spectrum may be due to the lack of a disk-star boundary layer and to the faintness of the short-wavelength continuum (see § 4). Or, alternatively, it may be due to our modest sensitivity: in order to detect even a narrow line (FWHM ~ 10 Å) at a 3 σ level of confidence would require a line luminosity of ~1.0 × 10^{30} ergs s^{-1}, which is ~10%–20% of the total X-ray luminosity (see § 2.4).

3.1.2. $\lambda < 2200$ Å

One indication of the reliability of the short-wavelength continuum can be made by comparing the grating and prism spectra in their range of overlap, 2200–2400 Å. In this range both dispersers are reasonably efficient and presumably well calibrated. We binned the data coarsely and found that the prism fluxes systematically exceed the grating fluxes by ~35%. We expect the prism fluxes to be more reliable than the grating fluxes because the coarser dispersion and greater efficiency of the prism reduce the importance of the background.

The level of the faint continuum shortward of 2200 Å is affected significantly by uncertainties in the background (see § 2.1). The averaged continuum spectrum is approximately flat between 1350 and 2200 Å (Fig. 4*b*): $f_\lambda \approx 1.0 \times 10^{-16}$ ergs s^{-1} cm^{-2} Å^{-1}. (We disregard the broad feature at 1300 Å; see Fig. 4*b* and caption.) How sensitive is this result to the choice of the region used to scale the standard background spectrum? Consider pixels 1–300 in Figure 1*a* and note that the average raw count rate in this interval clearly exceeds our adopted background spectrum. If one scales the STScI standard background spectrum to the average raw count rate recorded in pixels 1–300 (rather than 901–1200; see § 2.1), then the average 1350–2200 Å flux quoted above is reduced by a factor of ~5 to $f_\lambda \approx 0.2 \times 10^{-16}$ ergs s^{-1} cm^{-2} Å^{-1}. An inspection of Figure 1*a* indicates that this flux value represents a probable lower limit (corresponding to the highest background), whereas the average flux quoted earlier (for background pixels 901–1200) × 1.35 is approximately an upper limit. (The factor 1.35 corrects the grating spectrum to the level of the prism spectrum in their range of overlap.) *We therefore conclude that we have detected* A0620−00 *at an average flux of* $f_\lambda \approx (0.2\text{–}1.4) \times 10^{-16}$ ergs s^{-1} cm^{-2} Å^{-1} *in the wavelength range* 1350–2200 Å.

3.1.3. 9000 K *Blackbody Model*

The continuum spectrum of the accretion disk can be fitted approximately by the spectrum of a 9000 K blackbody reddened by $E(B-V) = 0.35$, as shown in Figure 5. The area of the model source (for $d = 1$ kpc) is only $A_{bb} = \pi(0.09\ R_\odot)^2$. The projected area of the disk, on the other hand, is much greater.

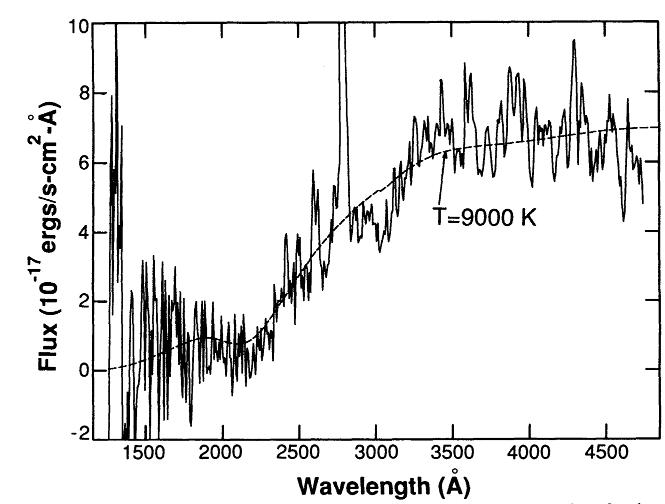

FIG. 5.—The spectrum of the accretion disk with no correction for interstellar reddening. The smooth curve represents the spectrum of the 9000 K blackbody model, which is described in the text. The feature at $\approx$1300 Å is an artifact (see the caption to Fig. 4*b*).

Analyses of the Hα spectroscopic data indicate that the radius of the disk is approximately half the radius of the Roche lobe of the compact object (Marsh et al. 1994). For $i \sim 65°$ and $M_x \sim 5\ M_\odot$ (Haswell et al. 1993), the projected area of the disk is $A_d \cos i \sim \pi(0.8\ R_\odot)^2$, which is ~ 80 times the area of the model blackbody source. The small size inferred for the latter suggests that it may be a bright spot in the stream-disk collision region. On the other hand, the continuum emission may come from an optically thin and extended region such as a torus of material located in the outer disk.

Additional information on the continuum flux is provided by the UV light curve (Fig. 2). It spans 1.08 orbital cycles and has a full amplitude of only 0.2 mag. There is no indication of a large-amplitude ($\Delta B \gtrsim 1$ mag) orbital hump in the light curve similar to those seen in many high-inclination quiescent dwarf novae (e.g., U Gem and IP Peg; Wood & Crawford 1986) where it is produced by the strongly anisotropic radiation from the bright spot. This may be seen as an argument against the interpretation mentioned above of the 9000 K blackbody component as bright-spot radiation.

3.2. *X-Ray Spectrum*

The observed X-ray luminosity is very modest, $L_x \approx 6 \times 10^{30}$ ergs s^{-1} ($d = 1$ kpc), and one must consider the possibility that it all may be generated in the corona of the rapidly rotating K5V secondary star ($v \sin i \approx 83$ km s^{-1}; Marsh et al. 1994). However, this appears to be unlikely. Studies of rapidly rotating K dwarfs indicate that L_x never exceeds 10^{30} ergs s^{-1}, whereas L_x(A0620−00) $> 3 \times 10^{30}$ ergs s^{-1} (90% confidence). Moreover, for the K dwarfs in the Pleiades there appears to be no dependence of L_x on $v \sin i$ (Eracleous, Halpern, & Patterson 1991, and references therein; Micela et al. 1994).

It therefore appears likely that most of the X-ray flux comes from the inner accretion disk (cf., Fu & Taam 1990). If we adopt the standard model for disk accretion, then the above luminosity implies a mass accretion rate of $\dot{M}_{\rm BH} \sim 2 \times 10^{-15}\ M_\odot$ yr^{-1} for a Schwarzschild black hole ($\epsilon = 0.06$) and $\dot{M}_{\rm BH} \sim 4 \times 10^{-16}\ M_\odot$ yr^{-1} for an extreme Kerr hole ($\epsilon \approx 0.30$; Thorne 1974). *We adopt the following upper limit* (90% *confidence*) *on the mass accretion rate into an assumed Schwarzschild black hole:* $\dot{M}_{\rm BH} < 5 \times 10^{-15}\ M_\odot$ yr^{-1}, 90% confidence (which corresponds to $L_x < 1.5 \times 10^{31}$ ergs s^{-1}; Fig. 3). The actual mass accretion rate may be much less if the black hole rotates rapidly or if the secondary star contributes significantly to the X-ray flux.

We note that the observed source temperature, $kT_x \approx 160$ eV, is much greater than would be expected if the accretion flow in the inner disk region is steady. For a steady, optically thick disk and a Schwarzschild metric, the maximum disk temperature for $M_{\rm BH} = 7\ M_\odot$ and $\dot{M}_{\rm BH} = 2 \times 10^{-15}$ is only ≈ 10 eV (Fu & Taam 1990), which is much cooler than the observed temperature of A0620−00 ($kT > 105$ eV; 90% confidence). This estimate suggests the possibility that there may be a far-UV and/or an EUV component of emission in addition to the soft X-ray component observed with *ROSAT*. However, the far-UV luminosity is very low: L(1350–2200 Å) = (0.2–1.4) $\times 10^{31}$ ergs s^{-1} (§ 3.1.2). Moreover, the absence of He II λ4686 line emission in the optical spectrum of A0620−00 rules strongly against the presence of any significant EUV luminosity. Optical observations made in 1992 January give a luminosity limit of $\lesssim 4 \times 10^{32}$ ergs s^{-1} for $55 < h\nu < 280$ eV (for $d = 1$ kpc, and $M_{\rm BH} = 3.7\ M_\odot$), which corresponds to a mass accretion rate of $\lesssim 1 \times 10^{-13}\ M_\odot$ yr^{-1} (Marsh et al. 1994).

Given that the X-ray and far-UV luminosities are each $\sim 10^{31}$, it is probable that the EUV luminosity is comparable. Thus, the total luminosity of ionizing radiation (X-ray + EUV + far-UV) is very probably less than 10^{32} ergs s^{-1}, or equivalently, less than 20% of the expected bolometric luminosity of the K5V secondary. Moreover, only a modest fraction of that radiation will be intercepted by the secondary star or the accretion disk. Thus, the results of optical observations are unlikely to be affected significantly by the reprocessing of ionizing photons.

4. DISCUSSION

The *optical luminosity* from the outer accretion disk of A0620−00 is most probably generated by viscous heating; this is also true of CVs. Therefore we can use A0620−00's disk luminosity ($M_v \approx 7$) and 7.8 hr orbital period, and the empirical relations derived for dwarf novae to estimate the rate of mass accretion onto the outer disk ($\dot{M}_d$) in A0620−00: we find $\dot{M}_d \sim 2 \times 10^{-10}\ M_\odot$ yr^{-1} (Warner 1987; his eq. 21). This value of M_d should be corrected downward for the ~ 7 times larger mass of the primary in A0620−00. For a steady state and optically thick disk the correction factor scales as $M_x^{1/4}$ in the Rayleigh-Jeans part of the spectrum, and as $M_x^{2/3}$ in the $\nu^{1/3}$ regime (Cheng et al. 1992); thus the correction factor is ~ 1.6–3.7. If the disk is optically thin, we are not aware of any simple scaling law. Moreover, the situation is more complicated if the disk is not steady, which is probably true for A0620−00 (as we argue below). In this case, one possibility is that the optical/UV emission is produced in a disk chromosphere powered by dynamo action (Horne & Saar 1991). Then the luminosity would be essentially independent of the mass of the central object. We conclude that the desired correction to $\dot{M}_d$ is uncertain but is probably less than an order of magnitude, and we choose to make no correction.

The above value for $\dot{M}_d$ is ~ 10 times the rate of mass transfer that is inferred from the energy released in the 1975 outburst ($\sim 3 \times 10^{44}$ ergs) and the 58 yr interval between outbursts: $\dot{M}_d \sim 3 \times 10^{-11}\ M_\odot$ yr^{-1} (McClintock et al. 1983). This estimate is based on the assumptions that the mass transfer rate is the same in outburst and in quiescence, and that no outbursts were missed between 1917 and 1975. We judge that this estimate and the one above are roughly comparable in reliability and for the purposes of the discussion below *we adopt the following average value for the mass accretion rate onto the outer disk*: $\dot{M}_d \sim 10^{-10}\ M_\odot$ yr^{-1}.

The *far-ultraviolet luminosity* of A0620−00 is modest compared to the *total* far-UV luminosities of dwarf novae in quiescence. To show this we use the dereddened fluxes of 11 dwarf novae at 1800 Å compiled by Verbunt (1987; his Table III), and the distance estimates given by Patterson (1984). These dwarf novae are listed in the column (2) of Table 2 (entries 1–11). One additional dwarf nova, OY Car, is also listed (entry 12), and is discussed separately below. The last entry is for A0620−00. For all of the objects, columns (3) and (4) give the type of object and the orbital period, respectively (Ritter 1990). Columns (5)–(7) give estimates for the distance, the reddening (Verbunt 1987), and the orbital inclination (Ritter 1990).

Column (8) contains the key quantity: the observed 1800 Å flux (corrected for reddening and) corrected by us to a uniform source distance of 1 kpc, which is the distance we have adopted for A0620−00. The fluxes have not been corrected for the effects of orbital inclination (e.g., Warner 1987); however, esti-

TABLE 2

DEREDDENED 1800 Å FLUXES REFERRED TO $D = 1$ KILOPARSEC

Entry Number (1)	Object (2)	Type (3)	P_{orb} (hr) (4)	d (pc) (5)	$E(B-V)$ (6)	i (7)	f_{1800} (10^{-16} ergs cm^{-2} s^{-1} $Å^{-1}$) (8)
1	VW Hyi	SU	1.8	150	0.0	60°	14.0
2	WX Hyi	SU	1.8	100	0.0	40	2.2
3	YZ Cnc	SU	2.1	130	0.0	38	4.0
4	CN Ori	ZC	3.9	400	0.0	67	18.0
5	U Gem	UG	4.2	78	0.0	70	3.1
6	RX And	ZC	5.0	200	0.0	51	30.0
7	HL CMa	ZC	5.1	80	0.10	45	4.4
8	SS Cyg	UG	6.6	95	0.04	37	14.0
9	Z Cam	ZC	7.0	350	0.0	57	96.0
10	EM Cyg	ZC	7.0	350	0.05	63	76.0
11	RU Peg	UG	9.0	250	0.0	33	40.0
12	OY Car	SU	1.5	120	0.0	83	0.2[a]
13	A0620−00	XT	7.8	1000	0.35	65[b]	0.2–1.4

[a] Eclipse observation; flux due solely to the accretion disk (Horne et al. 1994).
[b] A lower inclination angle, $i = 31°–54°$ (90% confidence), has been reported by Shahbaz, Naylor, & Charles 1994.

mates for the inclination angles are given in column (7) (for uncertainties, see Ritter 1990, and Haswell et al. 1993). Note that A0620−00 is less luminous than any of the 11 dwarf novae on Verbunt's list. However, this comparison is probably not a fair one because the flux at 1800 Å from a quiescent dwarf nova includes contributions from the white dwarf and boundary layer (which are absent for a black hole) as well as contributions from the bright spot and accretion disk. These various components of emission have been separated in the case of the eclipsing dwarf nova OY Car (entry 12; Horne et al. 1994). The bulk of the flux comes from the white dwarf. The flux from the disk alone (which is given in Table 2) is about one-sixth of the total flux; it is very comparable to the flux we observed from A0620−00 (entry 13), especially if one allows for the higher inclination of OY Car. *This comparison suggests that the low far-UV luminosity we observed for* A0620−00 *may be completely compatible with emission from a quiescent accretion disk similar to those present in quiescent dwarf novae.*

The *X-ray luminosity* of A0620−00 is much less than the quiescent luminosities of Cen X-4 and Aql X-1, two neutron star novae for which $L_x \gtrsim 5 \times 10^{32}$ ergs s^{-1} (Verbunt et al. 1994). Table 3 compares the quiescent luminosities of A0620−00 and two X-ray novae, GS 2000+25 and V404 Cyg, which are black hole candidates (van Paradijs & McClintock 1994). All three sources were observed at comparable sensitivity with the *ROSAT* PSPC detector for $\gtrsim 1.5 \times 10^4$ s. The upper limit on the luminosity of GS 2000+25 is comparable with the observed luminosity of A0620−00 (Verbunt et al. 1994). On the other hand, V404 Cyg is 1000 times more luminous than A0620−00 (Wagner et al. 1994).

X-ray emission is a key diagnostic of conditions in the very inner accretion disk and a direct measure of the mass transfer rate into the black hole ($\dot{M}_{BH}$). We noted in § 1 that de Kool (1988) attempted to reconcile the mass accretion rates inferred from optical observations and X-ray observations by attributing the X-ray faintness of A0620−00 to a low source temperature plus attenuation by the interstellar medium. The *ROSAT* observations do imply a fairly low temperature; however, the X-ray faintness is due primarily to the extraordinarily low luminosity of the source. The corresponding mass accretion rate, $\dot{M}_{BH} < 5 \times 10^{-15}$ $M_\odot$ yr^{-1}, and the accretion rate onto the outer disk, $\dot{M}_d \sim 10^{-10}$ $M_\odot$ yr^{-1}, obviously cannot be reconciled by de Kool's argument, or by any other steady state model.

There is, however, one ready model that can explain $\dot{M}_d > 2 \times 10^4 \dot{M}_{BH}$, and that is the disk instability model (e.g., see Cannizzo 1993, and references therein).[5] In the disk instability model (in simplest outline), matter is transferred from the secondary to the outer disk at a constant rate. However, instead

[5] An alternative model, in which the eruption is triggered by X-ray irradiation of the secondary, is less attractive. It is probable that A0620−00 with its relatively short orbital period has a convective envelope that is too massive to respond rapidly to X-ray illumination (Gontikakis & Hameury 1993).

TABLE 3

ROSAT PSPC OBSERVATIONS OF BLACK HOLE CANDIDATES IN QUIESCENCE

Source	ΔT (yr)[a]	d (pc)	kT_x Blackbody (keV)	N_H (10^{21} cm^{-2})	L_x (10^{30} ergs s^{-1})	References
A0620−00	16.6	1	0.16	1.6	≈6	1
GS 2000+25	4.0, 5.0	2	0.1[b]	1–2[c]	<24 (4 σ)[c]	2
			0.5[b]	1–2[c]	<10 (4 σ)[c]	
V404 Cyg	3.5	3.5	0.21	13	8000	3

[a] Time between nova outburst and observation.
[b] Assumed temperature.
[c] The value of N_H for GS 2000+25 adopted by Verbunt et al. 1994 is almost certainly too low. For example, Charles et al. 1991 report $A_V \sim 4$ mag or $N_H \sim 5 \times 10^{21}$, which would imply a significant increase in the upper limits on L_x given here.

REFERENCES.—(1) This work; (2) Verbunt et al. 1994; (3) Wagner et al. 1994.

of moving steadily inward to the central object, the matter accumulates at intermediate radii where the disk is cold and inviscid. Very gradually the density and opacity of the matter rises there, and eventually an unstable jump in temperature and viscosity occurs, which releases the stored matter onto the central object. This process, which is believed to occur in dwarf novae, can be repeated indefinitely as part of a limit cycle.

The disk instability model has been developed for A0620−00 in detail (Huang & Wheeler 1989; Mineshige & Wheeler 1989). The authors note the following successes of their model: it qualitatively reproduces the 58 year recurrence time, and the optical and X-ray outburst amplitudes and profiles, and it requires the large central mass of a black hole ($M_x \sim 10\ M_\odot$) in order to fit the long recurrence time. As an additional success, we confirm the model prediction that in quiescence less than 5×10^{-5} of the matter impinging on the outer disk makes its way to the black hole. A difficulty of the model, which is noted by the authors, is that both the model disk in quiescence and the hot spot are much too faint to account for the observed optical continuum. The results presented here do not solve this problem. Nevertheless, the results do provide strong support for the disk instability model both by demonstrating that $\dot{M}_{BH} < 5 \times 10^{-5} \dot{M}_d$ and that the inner regions of the quiescent disk are faint, as predicted.

5. HOW QUIET IS QUIESCENCE?

In quiescence, the inner accretion disk of A0620−00 is extraordinarily dormant. In the far-UV band, the luminosity is very low ($\lesssim 10^{31}$ ergs s^{-1}), and none of the common resonance lines (e.g., C IV λ1549) were detected. The quiescent X-ray luminosity is the lowest value that has been reported for any X-ray nova, and is only $\sim 5 \times 10^{-8}$ of the peak luminosity observed during the 1975 outburst (Elvis et al. 1975). Moreover, the total luminosity at short wavelengths (X-ray + EUV + far-UV) is unlikely to exceed 10^{32} ergs s^{-1} (§ 3.2). Radio observations, which are not discussed above, provide one additional measure of inactivity. During the 1975 outburst, A0620−00 was detected at 1400 and 2695 MHz at a flux density of 200–300 mJy (Owen et al. 1976). However, observations in quiescence during 1986 February with the VLA at 4.86 GHz failed to detect the source: $S_\nu < 0.3$ mJy (3 σ; Geldzahler 1987). Additional VLA observations at the same frequency in 1986 May by J. McClintock and L. Molnar yielded a stronger limit: $S_\nu <$ 0.14 mJy (3 σ).

Thus, despite the presence of a very strong gravitational field in the inner disk, we conclude that this region is remarkably quiet. In fact, the very inner disk may be somewhat less luminous than the outer disk, for which the 9000 K blackbody model (§ 3.1.3) implies $L_{bb} \sim 10^{32}$ ergs s^{-1}. Indeed, it is remarkable that there are probably *single* black holes accreting from clouds in the interstellar medium that are more luminous than A0620−00 in its quiescent state (Ipser & Price 1982; McDowell 1985).

We are grateful to Pierre Bely, Michael Eracleous, George Hartig, Ed Smith, and others at STScI for information on the detector background and telescope pointing, and to the staffs of the MDM Observatory and the MMT Observatory. We thank Keith Arnaud and Frank Primini for advice on analyzing the X-ray data, and Mark Birkinshaw, Paul Callanan, John Cannizzo, Josh Grindlay, and Craig Wheeler for comments on the manuscript. Support for this work was provided by NASA through grant number GO-2334 from the Space Telescope Science Institute and grant number NAG5-1982 from the *ROSAT* Guest Investigator Program. Additional support was provided to K. H. from NASA under grant NAGW-2678, and to J. E. M. from the Smithsonian Institution Scholarly Studies Program.

REFERENCES

Blair, W. P., Davidsen, A. F., & Uomoto, A. 1989, STScI Instrument Science Rept. CAL/FOS-058
Cannizzo, J. K. 1993, in Accretion Disks in Compact Stellar System, ed. J. C. Wheeler (Singapore: World Scientific), 6
Cardelli, J. A., Clayton, C. C., & Mathis, J. S. 1989, ApJ, 345, 245
Cash, W. 1979, ApJ, 228, 939
Charles, P. A., Kidger, M. R., Pavlenko, E. P., Prokofieva, V. V., & Callanan, P. J. 1991, MNRAS, 249, 567
Cheng, F. H., Horne, K., Panagia, N., Shrader, C. R., Gilmozzi, R., Paresce, F., & Lund, N. 1992, ApJ, 397, 664
de Kool, M. 1988, ApJ, 334, 336
Elvis, M., Page, C. G., Pounds, K. A., Ricketts, M. J., & Turner, M. J. L. 1975, Nature, 257, 656
Eracleous, M., Halpern, J., & Patterson, J. 1991, ApJ, 382, 290
Fu, A., & Taam, R. E. 1990, ApJ, 349, 553
Geldzahler, B. J. 1987, PASP, 99, 1036
Gontikakis, C., & Hameury, J. M. 1993, A&A, 271, 118
Gorenstein, P. 1975, ApJ, 198, 95
Haswell, C. A., Robinson, E. L., Horne, K., Stiening, R. F., & Abbott, T. M. C. 1993, ApJ, 411, 802
Haswell, C. A., & Shafter, A. W. 1990, ApJ, 359, L47
Heiles, C., Stark, A. A., & Kulkarni, S. 1981, ApJ, 247, L73
Horne, K., & Eracleous, M. 1993, STScI Instrument Science Report CAL/FOS-091
Horne, K., Marsh, T. R., Cheng, F. H., Hubeny, I., & Lanz, T. 1994, ApJ, 426, 1994
Horne, K., & Saar, S. H. 1991, ApJ, 374, L55
Huang, M., & Wheeler, J. C. 1989, ApJ, 343, 229
Ipser, J. R., & Price, R. H. 1982, ApJ, 255, 654
Jacoby, G. H., Hunter, D. A., & Christian, C. A. 1984, ApJS, 56, 257
Johnston, H. M., & Kulkarni, S. R. 1990, in Accretion Powered Compact Binaries, ed. C. W. Mauche (Cambridge: Cambridge Univ. Press), 17
Johnston, H. M., Kulkarni, S. R., & Oke, J. B. 1989, ApJ, 345, 492
Kinney, A. L. 1992, Faint Object Spectrograph Instrument Handbook, Version 2.0 (Baltimore: STScI), 10
la Dous, C. 1991, A&A, 252, 100
Long, K. S., Helfand, D. S., & Grabelsky, D. A. 1981, ApJ, 248, 925
Marsh, T. R., Robinson, E. L., & Wood, J. H. 1994, MNRAS, 266, 137
McClintock, J. E. 1986, in The Physics of Accretion onto Compact Objects, ed. K. O. Mason, M. G. Watson, & N. E. White (Berlin: Springer), 211
McClintock, J. E., Petro, L. D., Remillard, R. A., & Ricker, G. R. 1983, ApJ, 266, L27
McClintock, J. E., & Remillard, R. A. 1986, ApJ, 308, 110
———. 1990, BAAS, 21, 1206
McDowell, J. 1985, MNRAS, 217, 77
Micela, G., Sciortino, S., Kashyap, V., Harnden, F. R., Jr., & Rosner, R. 1995, ApJ, submitted
Mineshige, S., & Wheeler, J. C. 1989, ApJ, 343, 241
Murdin, P., Allen, D. A., Morton, D. C., Whelan, J. A. J., & Thomas, R. M. 1980, MNRAS, 192, 709
Oke, J. B. 1977, ApJ, 217, 181
Oke, J. B., & Greenstein, J. L. 1977, ApJ, 211, 872
Owen, F. N., Balonek, T. J., Dickey, J., Terzian, Y., & Gottesman, S. T. 1976, ApJ, 203, L15
Patterson, J. 1984, ApJS, 54, 443
Ritter, H. 1990, A&AS, 85, 1179
Shahbaz, T., Naylor, T., & Charles, P. A. 1994, MNRAS, 268, 756
Thorne, K. S. 1974, ApJ, 191, 507
van Paradijs, J., & McClintock, J. E. 1994, in X-Ray Binaries, ed. W. H. G. Lewin, J. van Paradijs, & E. P. J. van den Heuvel (Cambridge: Cambridge Univ. Press), in press
Verbunt, F. 1987, A&AS, 85, 1179
Verbunt, F., Belloni, T., Johnston, H. M., van der Klis, M., & Lewin, W. H. G. 1994, A&A, 285, 903
Wagner, R. M., Starrfield, S. G., Hjellming, R. M., Howell, S. B., & Kreidl, T. J. 1994, ApJ, 429, L25
Warner, B. 1987, MNRAS, 227, 23
Whelan, J. A. J., et al. 1977, MNRAS, 180, 657
Wood, J., & Crawford, C. S. 1986, MNRAS, 222, 645
Wu, C.-C., Crenshaw, D. M., Blackwell, J. H., Wilson-Diaz, D., Schiffer, F. H., III, Burstein, D., Fanelli, M. N., & O'Connell, R. W. 1991, NASA *IUE* Newsletter (*IUE* Ultraviolet Spectral Atlas), 43, 319
Wu, C.-C., Panek, R. J., Holm, A. V., Schmitz, M., & Swank, J. H. 1983, PASP, 95, 391